SECOND EUROPEAN CONFERENCE ON EARTHQUAKE ENGINEERING
AND SEISMOLOGY, ISTANBUL AUG. 25-29, 2014

"REAL-TIME" SEISMIC VULNERABILITY ASSESSMENT OF A HIGH RISE RC BUILDING USING FIELD MONITORING DATA

Sotiria KARAPETROU[1], Maria MANAKOU[2], Despoina LAMPROU[3], Sofia KOTSIRI[4], Kyriazis PITILAKIS[5]

ABSTRACT

In the framework of EU funded REAKT project (http://www.reaktproject.eu/) we evaluate the "real-time" seismic vulnerability of one of the main buildings of the most important hospital in Thessaloniki (AHEPA) using field monitoring data. The target building is an eight-storey RC structure composed by two units connected through a structural joint. The assessment of the dynamic characteristics is performed using ambient noise measurements recorded by a temporary seismic network installed inside the structure. System identification methods, namely the Frequency Domain decomposition and the Stochastic Subspace identification, are applied to perform operational modal analysis and extract the natural frequencies and mode shapes of the structural system. The modal identification results are used to update and better constrain the "initial" finite element model of the building, which is based on the available design and construction documentation plans. For both initial and updated finite element models, three-dimensional incremental dynamic analysis is performed to evaluate the actual seismic performance of the hospital building. Fragility curves are derived in terms of outcropping peak ground acceleration (PGA) for the immediate occupancy (IO) and collapse prevention (CP) limit states for the initial "as built" model and for the real structures as it is nowdays.

INTRODUCTION

Loss estimation and risk management presupposes the reliable vulnerability assessment of structures. Vulnerability is commonly expressed through fragility functions representing the probability of exceeding a prescribed level of damage for a wide range of ground motion intensities. Traditionally, in seismic vulnerability assessment studies it is implicitly assumed that the structures are optimally maintained during their lifetime neglecting any deterioration effect (e.g. aging, Pitilakis et al., 2014) that may adversely affect their structural performance under dynamic loading. Therefore the use of field monitoring data for identifying the actual state of the structures based on system identification techniques has drawn great attention in civil engineering community for developing real time assessment tools and reducing uncertainties involved in the risk assessment procedure (Michel et al., 2012).

Dynamic characterization of civil engineering structures (natural frequencies, damping ratios, mode shapes) becomes increasingly important in a wide range of research and application fields, such as dynamic response prediction (Brownjohn, 2003), finite element model updating (Teughels, 2003),

[1] PhD student, Aristotle University Thessaloniki, Thessaloniki, gkarapet@civil.auth.gr
[2] Dr, Aristotle University Thessaloniki, Thessaloniki, manakou@civil.auth.gr
[3] MSc, Aristotle University Thessaloniki, Thessaloniki, despina_31@hotmail.com
[4] MSc, Aristotle University Thessaloniki, Thessaloniki, kotsiris@civil.auth.gr
[5] Professor, Aristotle University Thessaloniki, Thessaloniki, kpitilak@civil.auth.gr

structural health monitoring and damage detection (Peeters, 2000). Rapid development of data acquisition and processing capabilities has given rise to major advances in the experimental operational studies and more specifically in the estimation of modal parameters of vibrating systems. Operational Modal Analysis (OMA) using ambient noise measurements is generally preferred due to the fact that the modal parameters can be obtained from vibration data in operational conditions.

In order to derive "real-time" fragility curves based on field monitoring data (e.g. ambient noise measurements) which correspond to the actual state and vulnerability of a structure, the measured modal parameters can be used to "correct" the finite element models to better reflect the measured data than the initial ones. The lack of correlation between the numerical structural models and experimental observations may be attributed to poorly known boundary conditions, unknown material properties or modeling simplifications. These uncertainties cause the predicted dynamics of a structure to be different from the measured dynamics of the real structure.

The present study aims at assessing the "real-time" seismic vulnerability of one of the main buildings of the most important hospital in Thessaloniki (AHEPA) based on field monitoring data. This RC building has been selected as test site for the European funded REAKT project (http://www.reaktproject.eu/). "Real-time" in this case means the present (actual) seismic vulnerability of the building considering all possible geometrical modifications, mass distributions and material deterioration. Ambient noise measurements are used to derive the mathematical model of the hospital building and identify its modal properties based on system identification and OMA respectively. The modal identification results are used to update and better constrain the "initial" finite element model of the building, which is based on the design and construction documentation plans provided by the Technical Services of the hospital in order to evaluate its real (actual) fragility and vulnerability. For both the initial and updated finite element models, incremental dynamic analysis is performed for 15 real ground motion accelerograms, corresponding to the regional seismic hazard, in order to derive the fragility curves and evaluate the actual state of the hospital building.

DESCRIPTION OF AHEPA HOSPITAL AND TEMPORARY INSTRUMENTATION ARRAYS

The AHEPA general hospital in Thessaloniki is one of the largest hospitals in northern Greece, located in the campus of Aristotle University. It is a major teaching and research center and part of the National Healthcare System of Greece. The target building hosts both administration and hospitalization activities. It was constructed in 1971 and is considered representative of structures that have been designed according to the old 1959 Greek seismic code ('Royal Decree' of 1959), where the ductility and the dynamic features of the constructions are ignored. It is an eight story infilled structure and its special feature is that it is composed of two adjacent tall building units that are connected with a structural joint (Fig. 1).

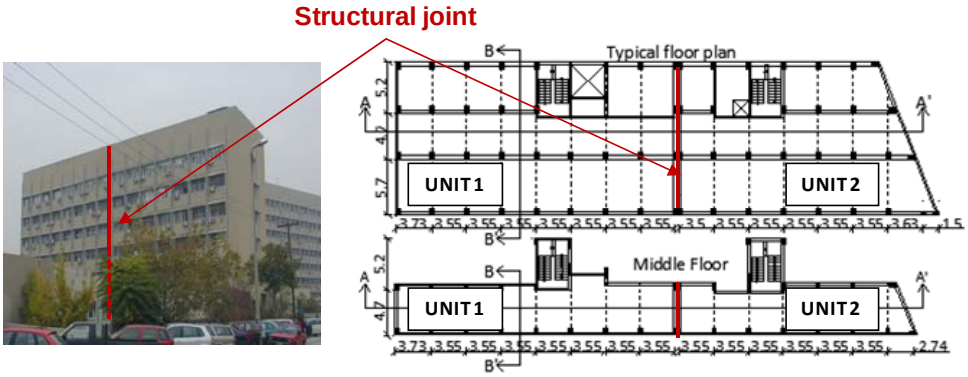

Fig. 1. Typical floor plan and middle floor with the structural joint

UNIT 1 covers a rectangular area of 29m by 16m while UNIT 2 has a trapezoidal cross section of 21m by 27m by 16m. The total height of the building with respect to the foundation level is 28.6m

with a constant inter-story height of 3.4m except for the second floor where the height increases to 4.8m due to the presence of a middle floor level which covers only a part of the typical floor plan (Fig. 1). From the structural point of view the building's force resisting mechanism comprises longitudinal and externally transverse reinforced concrete moment resisting frames (Fig. 1). The foundation system consists of simple footings of variable geometries without tie-beams combined partially with a raft foundation. Using the SYNER-G taxonomy (http://www.vce.at/SYNER-G/) for RC structures to describe the typology of the hospital building, it may be considered typical of high-rise infilled moment resisting frame buildings designed with low seismic code level. Table 1 presents the main characteristics of the two units, namely the mass, the strength of concrete, steel and masonry infill.

Table 1. Characteristics of the adjacent hospital units.

RC buildings	Total mass (t)	f_c (MPa)	f_y (MPa)	f_m (MPa)
UNIT 1	3719.0	14.0	220.0 and 500.0	3.0
UNIT 2	3112.0	14.0	220.0 and 500.0	3.0

In February 2013 a temporary array of 36 triaxial seismometrs was deployed in the hospital building in cooperation with GFZ Potsdam (http://www.gfz-potsdam.de/en/home/). In order to capture the translational and torsional modes of the building, the sensors were installed in every floor with the configuration illustrated in Fig. 2. Each floor was instrumented with four stations, which were installed along the middle corridor of the building near and far the structural joint (Fig. 2). The instruments were Mark Products short-period seismometers (L4C-3D, 1Hz natural frequency) coupled to EarthData recorders EDL (PR6-24). GPS antennas guaranteed common time of all instruments. North direction of the stations was placed parallel to the longitudinal structural direction of the building. Ambient noise was recorded simultaneously for about 4 hours in all stations with a sampling rate of 500 Hz and gain 10.

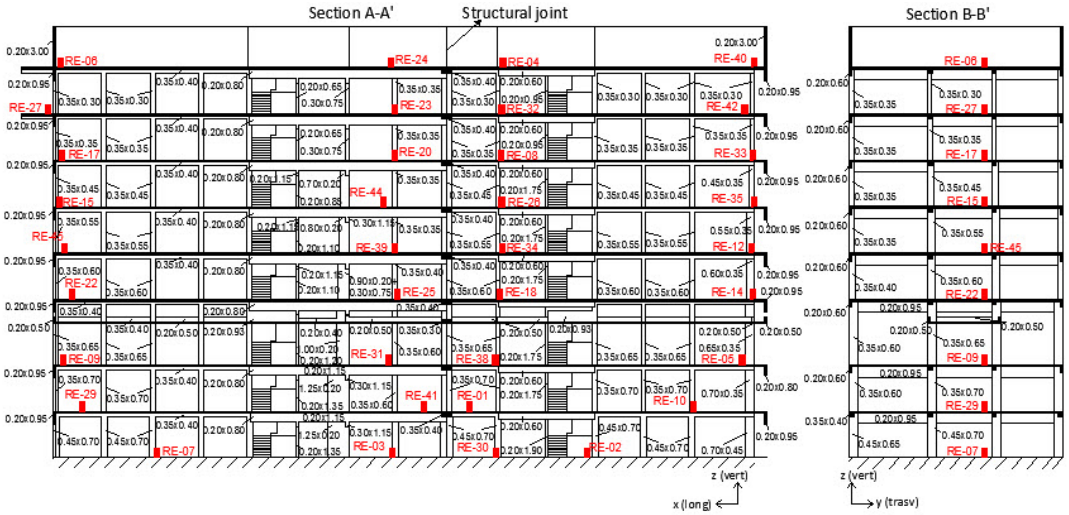

Fig. 2. Sections A-A´ and B-B´ along the longitudinal and transverse direction of the hospital building with the temporary instrumentation.

SYSTEM IDENTIFICATION AND OPERATIONAL MODAL ANALYSIS

To evaluate the dynamic characteristics of the hospital building, namely the natural frequencies and mode shapes, system identification and Operational Modal Analysis are performed using MACEC 3.2 software (Reynders et al., 2011) for the two adjacent building units separately (UNIT 1 and UNIT 2) as well as for the entire hospital building, analyzed as one taking into account the interaction of the two building units due to their connection with the structural joint (BUILDING). Operational modal analysis is conducted using only the horizontal components of the noise records. The grid of the models was built so that the defined nodes correspond to nodes that have been actually measured. The

stations that are used for the identification process are illustrated in Fig. 2. System identification and modal analysis of the structural models under study are conducted using non-parametric and parametric identification techniques, namely the Frequency Domain Decomposition-FDD (Brincker et al., 2001) and the Stochastic Subspace Identification-SSI (Van Overschee and De Moor, 1996) respectively. An advantage of the parametric over the non-parametric technique is the direct estimation of the system's damping ratio from the identification process. The results of the FDD and SSI analyses, namely the singular values and stabilization diagrams respectively, for the two adjacent buildings analyzed separately (UNIT 1 and UNIT 2) and as one single building (BUILDING) are presented in Fig. 3.

In Table 2, the eigenfrequencies computed with the two system identification methods are summarized. It is seen that the estimated frequency values for the five well separated modes are very close to each other (practically the same at the first three modes) for the two identification methods applied as well as for the different system models identified. Similar orders and shapes of the modes are estimated for the different system models implying that the dynamic interaction of the two adjacent buildings due to their connection with the structural joint is reflected on the measured outputs, and the dynamic characteristics of the complex hospital building is possible to be captured by monitoring and analyzing the two adjacent building units separately. Moreover the fact that frequencies and mode shapes are identical for both units may be attributed to their similar structural configuration. The building is exhibiting coupled sway and torsional modes in the frequency range of interest which are expected in case of geometric and structural irregularities or eccentricities between the center of mass and center of rigidity. The highly coupled obtained mode shapes confirm the complex vibrational characteristics of the building especially for the first two identified frequencies.

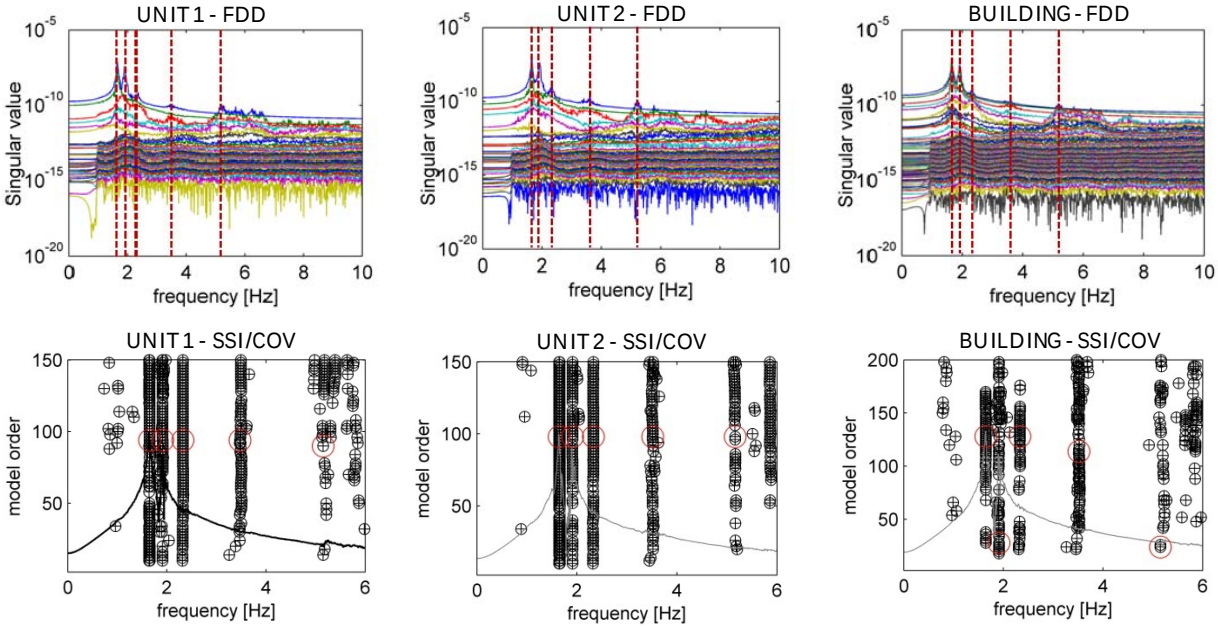

Fig. 3. Modal identification using the Frequency Domain Decomposition (FDD) and the reference-based covariance-driven Stochastic Subspace Identification (SSI-cov) method using ambient noise measurements.

Table 2. Modal identification results for UNIT 1, UNIT 2 and BUILDING estimated using parametric and non-parametric identification techniques.

Mode	Mode type	UNIT 1			UNIT 2			BUILDING		
		FDD (Hz)	SSI (Hz, ξ %)		FDD (Hz)	SSI (Hz, ξ %)		FDD (Hz)	SSI (Hz, ξ %)	
1	Coupled translational	1.65	1.65	0.8	1.65	1.65	0.9	1.65	1.65	0.8
2	Coupled translational	1.90	1.91	1.3	1.91	1.91	1.1	1.91	1.91	0.8
3	Torsional	2.33	2.33	3.6	2.35	2.33	3.5	2.35	2.33	3.2
4	1st Longitudinal	3.50	3.47	5.4	3.58	3.52	5.8	3.58	3.51	6.4
5	2nd Longitudinal	5.20	5.15	3.0	5.22	5.16	1.1	5.20	5.15	2.1

FINITE ELEMENT MODEL UPDATING

Model updating aims at the "correction" of the finite element model based on data processing, obtained from measurements conducted on the test structure (Mottershead and Friswell, 1993). The main purpose is to modify iteratively updating parameters to result in structural models that better reflect the measured data than the initial ones. One of the key issues during the updating process is the selection of the appropriate updating parameter. In general structural features, such as material properties, mass and geometry are likely to be selected as updating parameters in order to increase the correlation between the observed dynamic response of the structure and the predicted from the numerical model (Scodeggio et al., 2012). The aim of the procedure is to conduct an extensive parametric study of the hospital buildings considering the variation in structural parameters (e.g. modulus of elasticity), investigating the sensitivity of the model to material properties, and how the latter may affect the overall stiffness of the structure.

The "initial" numerical model of the buildings under study is based on the design and construction documentation plans provided by the Technical Services of the hospital. The numerical modeling is conducted for the two adjacent units separatly using OpenSees finite element platform (Mazzoni et al., 2009). Elastic beam-column and truss elements are employed to model the linear RC elements (beams and columns) and masonry infills respectively. For the linear modeling of the masonry infills a double strut model is adopted to represent the in-plane behavior of the infill panel. Fixed base conditions are assumed for both structural models.

For the updating procedure the compressive strength of the masonry infill f_m is selected as sensitivity parameter to take into account the uncertainties of the material behavior as well as the possible heterogeneity between the material properties of the different infill parts. A suite of numerical models is generated considering a proper distribution for f_m and defining possible scenarios adopting different infill masonry compressive strength values and configurations (Scodeggio et al., 2012). The mean value of the masonry compressive strength μ=3MPa and its covariance COV=20% are defined based on a normal distribution according to (Mosalam et al., 1997). The different values of compressive strength for the considered updating scenarios are subsequently computed based on the mean and standard deviation s according to the adopted normal distribution considering a limit range for the mean value of μ-3s≤f_m≤μ+3s. Then the elastic modulus in compression, which is used as input parameter to simulate the masonry infills, is estimated based on the adopted mean value for the compressive strength according to the relation E_m= 1000f_m (Paulay and Priestley, 1992). Five different scenarios are investigated regarding the variation in E_m and the considered configurations of the masonry infills for the selection of the 'best' model as illustrated in Fig. 4.

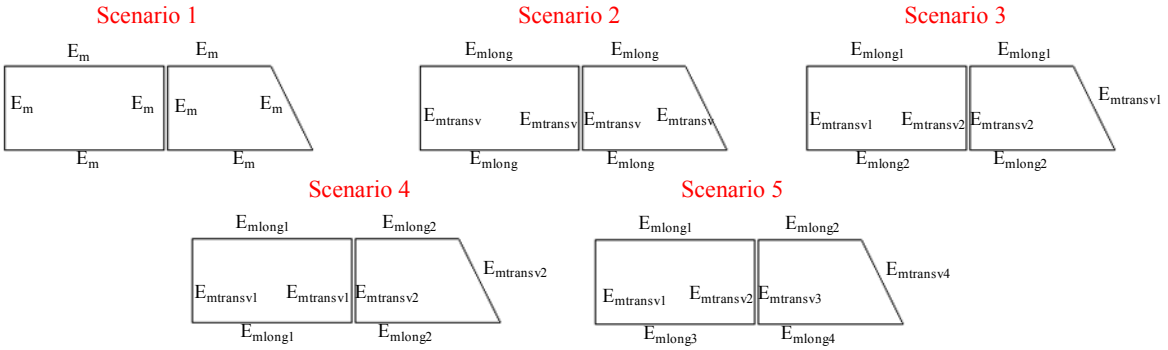

Fig. 4. The different updating scenarios adopted within this study.

Modal analyses for all the derived numerical models are performed in OpenSees for the three dimensional elastic linear finite element models of the two adjacent buildings separately (UNIT 1 and UNIT 2). Only one among them is considered as the 'best' model representing the observed dynamic response based on the ambient noise measurements. The selection of the 'best' model is made based on the evaluation of the Modal Assurance Criterion (MAC) defined as:

$$MAC_{ij} = \frac{\left(\varphi_j^T \varphi_{Ei}\right)}{\left(\varphi_j^T \varphi_i\right)\left(\varphi_{Ei}^T \varphi_{Ei}\right)} \quad (1)$$

where φ_j is the eigenvector j from numerical model and φ_{Ei} the eigenvector i from field monitoring test. A good correlation between the two tested modes is considered to be achieved for MAC values greater than 0.8. The scenario that represents most accurately the experimental results for the modes under investigation is found to be the one corresponding to the updating scenario 3. The elastic moduli in compression of masonry infills adopted for this scenario were the following: E_{mlong1}= 3GPa (f_m=μ=3MPa), E_{mlong2}=1.8GPa (f_m=μ-2σ=1.8MPa), $E_{mtransv1}$=3GPa (f_m=μ=3MPa) and $E_{mtransv2}$=4.8GPa (f_m=μ+3σ=4.8MPa). It should be noted herein that only the first three modes are considered in the updating process, which activate approximately 80% of the total mass of the buildings.

In Tables 3 and 4 the results of the updating methodology for UNIT 1 and UNIT 2 are presented respectively. The eigenfrequencies and mode shapes of the updated finite element models are compared to the initial ones as well as to the experimental results. It is seen that for UNIT 1 the updated finite element model correlates well with the experimental results for all the modes under investigation (MAC>0.8). For UNIT 2 on the other hand, MAC values are high for the 1st and 3rd mode, indicating the satisfactory correlation between analytically and experimentally calculated modal parameters, whereas for the 2nd mode it was not possible to achieve MAC values greater than 0.8. This may be attributed to the fact that the structural configuration of UNIT 2 did not allow to capture the 2nd mode shape, probably because another sensitivity parameter related not to the structural stiffness (such as the masonry compressive strength) but to the storey mass or a combination of several parameters related to both stiffness and mass, would be more appropriate.

INELASTIC FINITE ELEMENT MODELING

The numerical modeling of the structure is conducted using OpenSees finite element platform (Mazzoni et al., 2009). Inelastic force-based formulations are employed for the simulation of the nonlinear three-dimensional with six degrees of freedom beam-column frame elements. The applied formulations allow both geometric and material nonlinearities to be captured. Distributed material plasticity along the element length is considered based on the fiber approach to represent the cross-sectional behavior. Each fiber is associated with a uniaxial stress-strain relationship; the sectional stress-strain state of the beam-column elements is obtained through the integration of the nonlinear uniaxial stress-strain response of the individual fibers in which the section is subdivided. The Popovics (1973) concrete model is used to define the behavior of the concrete fibers, yet different material parameters are adopted for the confined (core) and the unconfined (cover) concrete. The uniaxial 'Concrete04' material is used to construct a uniaxial Popovics concrete material object with degraded linear unloading/reloading stiffness according to the work of Karsan and Jirsa (1969) with zero tensile strength. The steel reinforcement is modeled using the uniaxial 'Steel01' material to represent a uniaxial bilinear steel material with kinematic hardening described by a nonlinear evolution equation. For the nonlinear modelling of the masonry infills inelastic struts are used to represent infill walls because they have sufficient accuracy to capture key characteristics of force-displacement response. Each strut is assigned an elasto-plastic force displacement relationship representing initial stiffness and peak strength behavior of the masonry. To take into account the rigidity against the in-plane deformation of the floor slabs, diaphragm constraint is employed. For both structural models fixed base conditions are assumed.

SELECTION OF THE INPUT MOTION

A representative set of accelerograms is selected that is subsequently used for non-linear incremental dynamic analysis to provide the necessary response for the derivation of fragility curves. The selected scenario earthquake consists of a set of 15 real ground motion records (Table 5) obtained from the European Strong-Motion Database (http://www.isesd.hi.is). They are all referring to stiff soil conditions classified as soil type B according to EC8 with moment magnitude (M_w) and epicentral distance (R) that range between $5.8<M_w<7.2$ and $0<R<45$km respectively. In order to eliminate potential source of bias in structural response, the selection of pulse-like records is avoided. The primary selection criterion was the average acceleration spectra of the set to be of minimal "epsilon"

Table 3. Comparison of the updated finite element model of UNIT 1 with the initial model and the experimental results.

Initial FEM T (sec)/f(Hz)	Mode shape of updated FEM T (sec)/f(Hz)	Mode shape of experimental model T(sec)/f(Hz)	MAC
Coupled translational T_1=0.69sec/f_1=1.46Hz	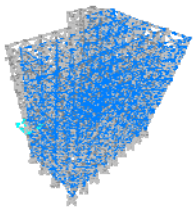	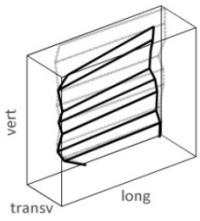	0.96
	T_1=0.64sec/f_1=1.56Hz	T_1=0.61sec/f_1=1.65Hz	
Coupled translational T_2=0.48sec/f_2=2.06Hz	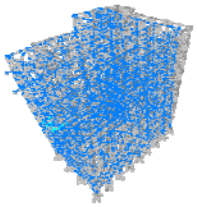	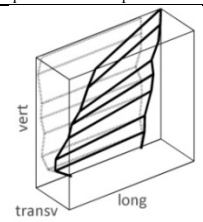	0.94
	T_2=0.53sec/f_2=1.89Hz	T_2=0.52sec/f_2=1.91Hz	
Torsional T_3=0.37sec/f_3=2.66Hz	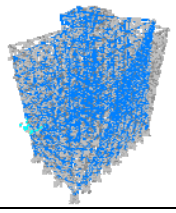	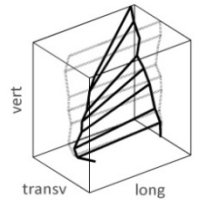	0.97
	T_3=0.37sec/f_3=2.70Hz	T_3=0.43sec/f_3=2.33Hz	

Table 4. Comparison of the updated finite element model of UNIT 2 with the initial model and the experimental results.

Initial FEM T (sec)/f(Hz)	Mode shape of updated FEM T (sec)/f(Hz)	Mode shape of experimental model T(sec)/f(Hz)	MAC
Coupled translational T_1=0.67sec/f_1=1.50Hz	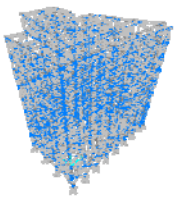	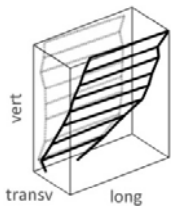	0.98
	T_1=0.65sec/f_1=1.54Hz	T_1=0.61sec/f_1=1.65Hz	
Coupled translational T_2=0.49sec/f_2=2.05Hz	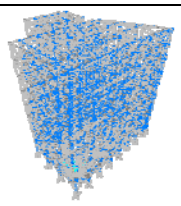	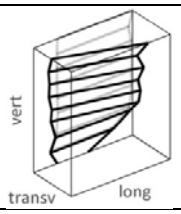	<0.8 due to the particular structural configuration
	T_2=0.53sec/f_2=1.89Hz	T_2=0.52sec/f_2=1.91Hz	
Torsional T_3=0.36sec/f_3=2.77Hz	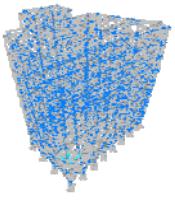	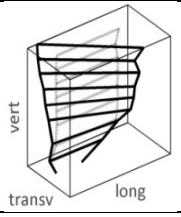	0.94
	T_3=0.35sec/f_3=2.86Hz	T_3=0.43sec/f_3=2.33Hz	

(Baker and Cornell, 2005) at the period range of 0.00<T<2.00sec with respect to the acceleration spectrum adopted from SHARE for a 475 year return period (http://portal.share-eu.org:8080/jetspeed/portal/). The optimization procedure was performed making use of the REXEL software (Iervolino et al., 2010). Fig. 5 depicts the mean normalized elastic response spectrum of the records in comparison with the corresponding reference spectrum adopted from SHARE. As shown in this Fig. 5, a good match between the two spectra is achieved.

Table 5 List of records used for the IDA.

Earthquake Name	Station ID	Date	M_w	R [km]	PGA_X [m/s^2]	PGA_Y [m/s^2]	Waveform ID
Friuli (aftershock)	ST28	15/9/1976	6.0	14	1.3841	2.3189	000147
Izmit (aftershock)	ST3265	13/9/1999	5.8	23	1.8983	1.2837	006959
Montenegro (aftershock)	ST76	24/5/1979	6.2	21	1.6273	1.3034	000231
South Iceland	ST2488	17/6/2000	6.5	17	3.9202	2.3852	004676
Kalamata	ST164	13/9/1986	5.9	10	2.1082	2.9095	000413
Izmir	ST162	6/11/1992	6.0	41	0.6527	0.8007	000549
Potenza	ST99	3/2/1998	5.8	36	0.7848	0.8544	000944
Ano Liosia	ST1101	7/9/1999	6.0	17	1.171	1.0661	001314
Tithorea	ST166	18/11/1992	5.9	25	0.3709	0.2744	000550
Ano Liosia	ST1258	7/9/1999	6.0	14	2.3842	2.1588	001714
South Aegean	ST1310	23/5/1994	6.1	45	0.5976	0.4023	001881
Ano Liosia	ST1255	7/9/1999	6.0	20	0.8549	0.7604	001711
Valnerina	ST83	19/9/1979	5.8	39	0.3855	0.2303	000244
Friuli (aftershock)	ST35	15/9/1976	6.0	21	4.6466	4.9562	000126
Duzce 1	ST3134	36476	7.2	11	1.0914	0.7137	006494

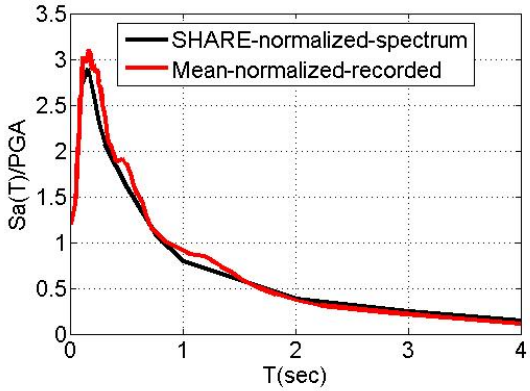

Fig. 5. Normalized average elastic response spectrum of the input motions compared with the corresponding reference spectrum adopted from SHARE.

INCREMENTAL DYNAMIC ANALYSIS IDA

The IDA procedure (Vamvatsikos and Cornell, 2002) is used to determine the seismic performance and assess the seismic vulnerability of the initial and updated finite element models of UNIT 1 and UNIT 2. Within this study the damage measure is expressed in terms of maximum inter-storey drift ratio, maxISD. More specifically the maximum peak SRSS drift (i.e. the maximum over all stories of the peak of the square-root-sum-of-squares of each storey's drift) in the two principal directions is selected (Wen and Song, 2002). The seismic intensity is described using peak ground acceleration (PGA) recorded on rock outcropping or soil type A according to EC8.

IDA is conducted for the structural models by applying the 15 progressively scaled records. In particular, we apply a PGA-stepping tracing algorithm for each record with an initial step of 0.1 g, a step increment of 0.1g and a first elastic run at 0.05g. It should be noted that for certain records it was necessary to reduce the step size of the algorithm to increase the accuracy close to the flatline of the IDA curve. To obtain reliable results for the derivation of the IDA curves, the minimum number of

converging runs is allowed to vary from 10 to 15 per record depending on the characteristics of the structure and the record itself.

By interpolating the derived pairs of PGA and maxISD for each individual record 15 continuous IDA curves for each structural model are derived. Fig. 6 illustrates representantive IDA curves for each record in terms of PGA for the updated finite element models of UNIT 1 and UNIT 2. For the purpose of the present study, two limit states are defined in terms of maximum inter-story drift ratio, maxISD, representing the immediate occupancy (IO) and collapse or near collapse prevention (CP) performance levels. For both initial and updated models, the first limit state is defined at 0.1% according to HAZUS prescriptions (NIBS, 2004) for RC moment resisting frame structures, whereas the second is assigned at a point where the IDA curve is softening towards the flat line (Fig. 6), but at low enough values of maxISD so that we still trust the structural model. Thus different CP limit state values are chosen on the IDA curves for the same structure depending on the reference finite element model (initial or updated) and the individual record. Finally the median of the defined CP limit states in terms of SRSS inter-storey drift is used to define the CP limit state of the structure, which for both structures is found to be equal to 1.4% and 1.1% for the initial and updated models respectively.

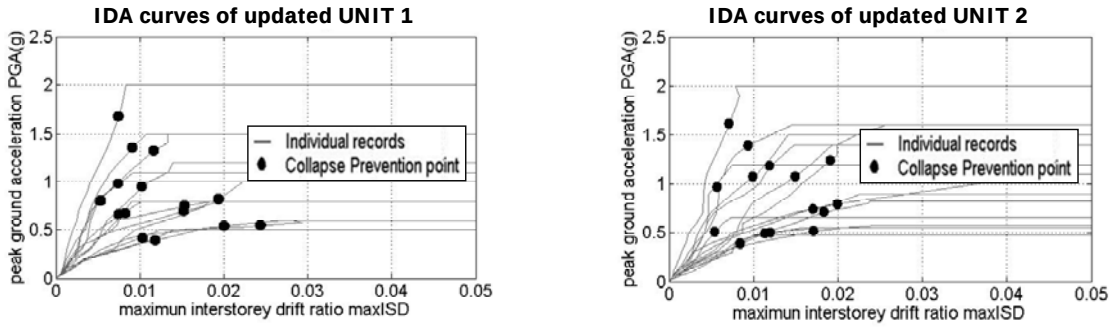

Fig. 6. Assignments of the CP limit damage state points on the IDA curves for the updated units.

DERIVATION OF FRAGILITY CURVES

A fragility curve represents a graphical relationship of the probability of exceeding a predefined level of damage (e.g. IO, CP) under a seismic excitation of a given intensity. The results of the IDA (PGA - maxISD values) are used to derive the fragility curves for both analyzed buildings, expressed as a two-parameter lognormal distribution functions. Equation 2 gives the cumulative probability of exceeding a damage state *DS* conditioned on a measure of the seismic intensity *IM*.

$$P[DS / IM] = \Phi\left(\frac{In(IM) - In(\overline{IM})}{\beta}\right) \quad (2)$$

where, Φ is the standard normal cumulative distribution function, *IM* is the intensity measure of the earthquake expressed in terms of PGA (in units of *g)*, $\overline{IM}$ and β are the median values (in units of *g)* and log-standard deviations respectively of the building fragilities and *DS* is the damage state. The median values of PGA corresponding to the prescribed performance levels are determined based on a regression analysis of the nonlinear IDA results (PGA- maxISD pairs) for both buildings. More specifically a linear regression fit of the logarithms of the PGA- maxISD data which minimizes the regression residuals is adopted in all analysis cases. Fig. 7 presents the PGA - maxISD relationships for the updated models of both UNIT 1 and UNIT 2, where it is noticed that the results show similar distribution and curve fitting.

The various uncertainties are taken into account through the log-standard deviation parameter β(t), which describes the total dispersion related to each fragility curve. Three primary sources of uncertainty contribute to the total variability for any given damage state (NIBS, 2004), namely the variability associated with the definition of the limit state value, the capacity of each structural type and the seismic demand. The log-standard deviation value in the definition of limit states is assumed to be equal to 0.4 while the corresponding value in the capacity is assumed to be 0.3 for the low code

structures (NIBS, 2004). The third source of uncertainty associated with the demand, is taken into consideration by calculating the dispersion of the logarithms of PGA - maxISD simulated data with respect to the regression fit. Under the assumption that these three log-standard deviation components are statistically independent, the total log-standard deviation is estimated as the root of the sum of the squares of the component dispersions. The herein computed log-standard deviation β values of the curves vary from 0.72 to 0.79 for the considered finite element models of the adjacent building units.

Fragility curves are derived for the initial and updated finite element models of UNIT 1 and UNIT 2. The initial "as built" numerical models are based on the available design plans and correspond to the initial state of the structures, whereas the updated models reflect the measured responses and therefore represent their actual state. The calculated fragility curves of UNIT 1 and UNIT 2 that corrspond to their initial state have been compared with the literature (Kappos et al., 2003 and 2006) in Fig. 8. A good agreement between the curves is observed verifying the reliability of the derived fragility functions for the hospital building units. The "real"-time fragility curves are obtained by assessing the seismic performance of the updated numerical models and are compared with the initial ones in Fig. 9. The updated curves present a shift to the left in comparison to the initial ones, indicating an increase in the structures vulnerability which is more noticeable for the CP limit state and for large intensities. Furthermore it can be seen that the derived curves are similar for the two buildings, which can be attributed to their similar structural configuration, stiffness and mass properties. Table 6 presents the lognormal distributed fragility parameters (median and log-standard deviation) in terms of PGA for the initial and updated models of UNIT 1 and UNIT 2 respectively.

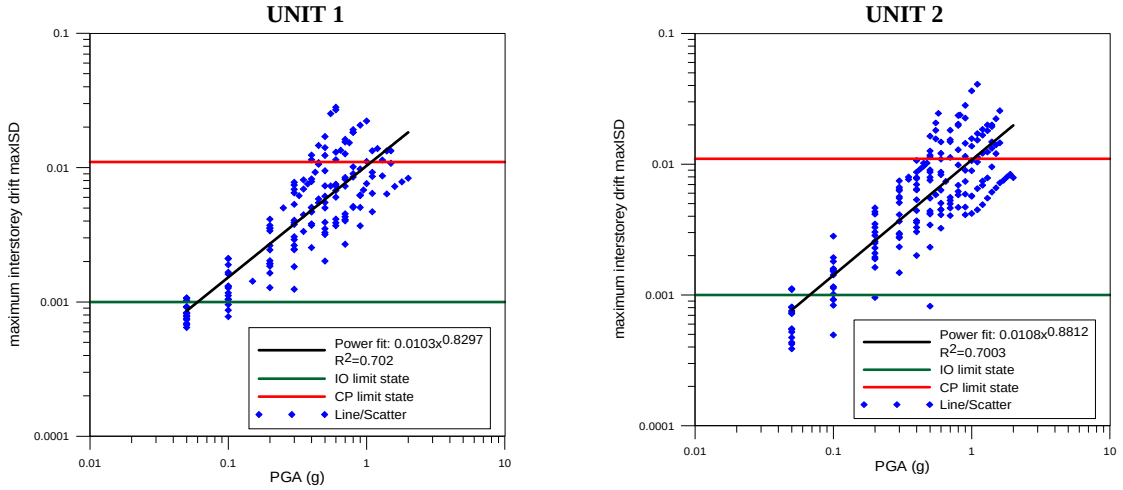

Fig. 7. PGA-maxISD relationships for updated finite element models of UNIT 1 and UNIT 2.

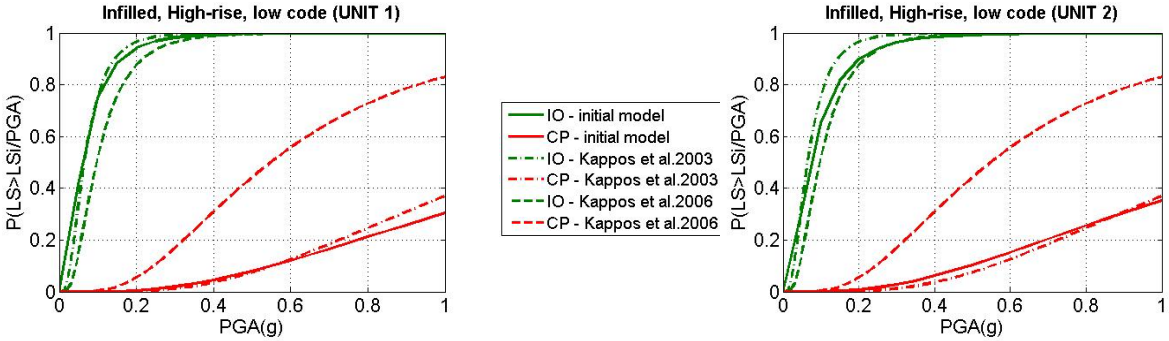

Fig. 8. Comparative plots of the "initial" fragility curves derived for the two adjacent building units with the corresponding fragility curves provided by Kappos et al. (2003 and 2006).

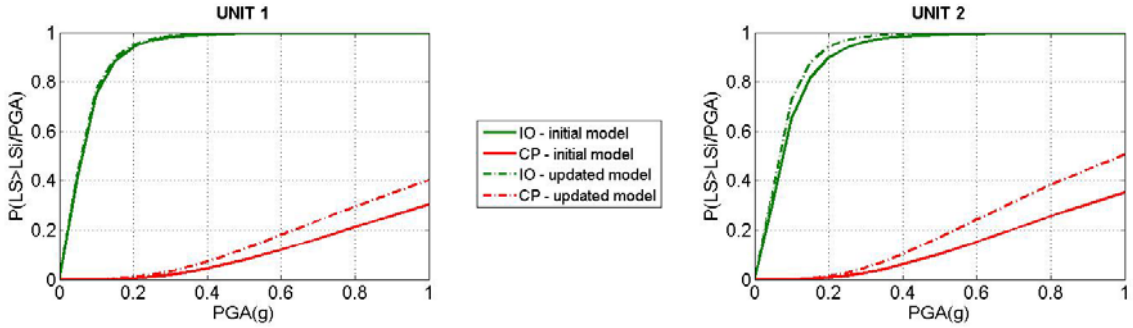

Fig. 9. Comparative plot of the fragility curves derived for the initial and updated models of UNIT 1 & UNIT 2.

Table 6. Parameters of the derived fragility curves for the initial and updated finite element models for UNIT 1 and UNIT 2.

RC building	Finite Element Model	Median PGA (g)		Dispersion
		IO	CP	
UNIT 1	Initial	0.059	1.62	0.78
	Updated	0.057	1.21	0.76
UNIT 2	Initial	0.74	1.45	0.79
	Updated	0.065	0.99	0.72

CONCLUSIONS

The "real-time" or "actual" seismic vulnerability of one of the main buildings of the most important hospital in Thessaloniki (AHEPA) has been assessed based on field monitoring data. The special feature of the target building is that it is composed of two adjacent tall units that are connected with a structural joint. Ambient noise measurements were used to derive the mathematical model of the two adjacent buildings first separately, and then for the entire building analyzed as one taking into account the interaction of the two building units and identify their modal properties based on system identification and OMA respectively. The identified modal parameters were similar for the different identification methods (non-parametric and parametric) applied as well as for the different system models analyzed, implying that the dynamic characteristics of the hospital building analyzed as one are possible to be captured by monitoring and analyzing only the two adjacent buildings separately.

The modal identification results were used to update and better constrain the "initial" finite element models of the two adjacent units, which were based on the design and construction documentation plans provided by the Technical Services of the hospital. A sensitivity parameter related to the structural stiffness was adopted for the updating procedure, namely the compressive masonry infill strength. While in general a very good correlation with the experimental results was achieved for the two adjacent buildings using this sensitivity parameter, it became evident that a combination of several parameters related to both stiffness and mass would probably be more appropriate to encounter an even better matching between experimental and numerical response for both low and high modes.

Incremental dynamic analysis was performed for the initial and updated structural models to evaluate the seismic perfomance of the buildings when their actual state is taken into account. The fragility functions were derived for the IO and CP limit states in terms of PGA for both units. An overall increase in structures fragility for the updated models is observed in comparison to the ones corresponding to their initial state and are currently used so far. Thus the present study provides further insight on the assessment of the "real-time" seismic vulnerability of typical RC buildings using field monitoring data, taking into account the actual state of the structure (degradation due to time, possible pre-existing damages, changes in geometry and mass distribution, etc). The proposed updating methodology can be used to yield more reliable structural models with respect to their real conditions in terms of structural detailing, mass distribution and material properties. Furthermore the proposed methodology could be extended for "real-time" risk assessment and post-seismic fragility updating.

ACKNOWLEDGMENTS

The work reported in this paper was carried out in the framework of the ongoing REAKT (http://www.reaktproject.eu/) project, funded by the European Commission, FP7-282862. The 36 seismometers (L4C-3D, 1Hz natural frequency) with the accompanied digitizers (EarthData recorders EDL, PR6-24) and the GPS antennas were kindly provided by the GFZ Potsdam laboratory in the frame of the REAKT project (http://www.gfz-potsdam.de/en/home/). We thank the GFZ team and AUTH team for their valuable help during the experiment and Assistant Professor Dimitris Pitilakis for his contribution to this research work.

REFERENCES

Baker JW, Cornell CA (2005) "A vector valued ground motion intensity measure consisting of spectral acceleration and epsilon," *Earthquake Engineering and Structural Dynamics*, 34:1193-1217.

Brincker R, Zhang L, Andersen P (2001) "Modal identification of output only systems using frequency domain

Brownjohn JMW (2003) "Ambient vibration studies for system identification of tall buildings", *Earthquake Engineering Structural Dynamics* 32: 71-95.

Iervolino I, Galasso C, Cosenza E (2010) "REXEL: Computer aided record selection for code-based seismic structural analysis," *Bulletin of Earthquake Engineering*, 8: 339-362.

Kappos AJ, Panagiotopoulos C., Panagopoulos G, Panagopoulos El, (2003) WP4-Reinforced concrete buildings (Level I and II analysis), RISK-UE: An advanced approach to earthquake risk scenarios with applications to different European towns.

Kappos AJ, Panagopoulos G, Panagiotopoulos C, Penelis G. "A Hybrid Method for the Vulnerability Assessment of R/C and URM Buildings", *Bulletin of Earthquake Engineering* 4(2006) 391-419.

Karsan I and Jirsa J (1969) "Behavior of Concrete under Compressive Loadings", ASCE Journal of the Structural Division 95:2543-2563.

Mazzoni S, McKenna F, Scott MH, Fenves GL (2009) Open System for Earthquake Engineering Simulation User Command-Language Manual, Pacific Earthquake Engineering Research Center, Berkeley, California.

Michel C, Guéguen P and Causse M (2012) "Seismic Vulnerability Assessment to Slight Damage based on Experimental Modal Parameters", *Earthquake Engineering and structural dynamics* 41: 81-98.

Mosalam KM, White R.N. and Gergely P (1997) "Static Response of Infilled Frames Using Quasi-Static Experimentation", ASCE Journal of Structural Engineering 123.

Mottershead JE and Friswell MI (1993) "Model Updating in Structural Dynamics: A Survey", *Journal of Sound and Vibration* 167.

National Institute of Building Sciences NIBS (2004) Direct physical damage – General building stock, HAZUS-MH Technical manual, Chapter 5, Federal Emergency Management Agency, Washington, D.C.

Paulay T and Priestle M (1992) Seismic Design of Reinforced Concrete and Masonry Buildings, New York.

Peeters B (2000) System Identification and Damage Detection in Civil Engineering, PhD thesis, Department of CivilEngineering, K.U.Leuven.

Pitilakis KD, Karapetrou ST, Fotopoulou SD (2014) "Consideration of aging and SSI effects on seismic vulnerability assessment of RC buildings", *Bulletin of Earthquake engineering*, Doi 10.1007/s10518-013-9575-8.

Popovics S (1973) "A Numerical Approach to the Complete Stress Strain Curve for Concrete", *Cement and concrete research*, 3(5): 583-599.

Reynders E, Schevenels M, De Roeck G. (2011) MACEC 3.2: A Matlab toolbox for experimental and operational modal analysis-User's manual, Katholieke Universiteit, Leuven 2011.

Scodeggio A, Monteiro R., Daccaro F, Crowley H, Pinho R (2012) "Finite Element Model Updating of Buildings using Dynamic Identification Measurements" *Proceedings of 15th World Conference on Earthquake Engineering*, Lisboa.

Teughels A (2003) Inverse modeling of civil engineering structures based on operational modal data, PhD thesis, Katholieke Universiteit of Leuven.

Vamvatsikos D and Cornell CA (2002) "Incremental dynamic alanysis", *Earthquake Engineering and Structural Dynamics* 31.

Van Overschee P and De Moor B (1996) Subspace Identification for Linear Systems: Theory-Implemantation-Applications, K.U.Leuven Academic Publishers.

Wen YK and Song SH (2002) "Structural reliability/redundancy under earthquakes", *ASCE Journal of Structural Engineering* 129: 56–67.